

# Mechanical properties and tuning of three-dimensional polymeric photonic crystals

Saulius Juodkazis, Vyngantas Mizeikis, Kock Khuen Seet, and Hiroaki Misawa<sup>a)</sup>

Research Institute for Electronic Science, Hokkaido University, CRIS Bldg., Sapporo 001-0021, Japan

Ulrike G. K. Wegst

Department of Materials Science and Engineering, Drexel University, 3141 Chestnut Street, Philadelphia, Pennsylvania 19104, USA

(Received 20 October 2007; accepted 19 November 2007; published online 11 December 2007)

Mechanical properties of photopolymerized photonic crystal (PhC) structures having woodpile and spiral three-dimensional architectures were examined using flat-punch indentation. The structures were found to exhibit a foamlite response with a bend-dominated elastic deformation regime observed at strain levels up to 10%. Numerical simulations of optical properties of these PhC structures demonstrate the possibility of achieving a substantial and reversible spectral tuning of the photonic stop gap wavelength by applying a mechanical load to the PhC.

© 2007 American Institute of Physics. [DOI: 10.1063/1.2822825]

Laser-induced photopolymerization in liquid resins and solid photoresists attracts significant interest due to its applicability for the fabrication of three-dimensional (3D) microstructures. The recording of 3D microstructures consisting of submicrometer sized features was demonstrated using direct laser writing (DLW).<sup>1-3</sup> DLW can be used for the preparation of elements of microfluidic and microelectromechanical systems, such as molecular sieves, thermal isolators, microdampers, and optomechanical converters.<sup>4,5</sup> Spatially periodic polymeric microstructures can be utilized in photonics and optoelectronics as photonic crystals (PhC) for the control of optical phenomena via photonic band gap (PBG) and photonic stop-gap (PSG) effects.

Many of these applications would benefit from the possibility of dynamic and reversible adjustments of the structures' parameters. For example, in PhC structures the central wavelength of the PBG or PSG intervals scales with the lattice period.<sup>6</sup> An elastic deformation of the PhC would modify the lattice period and tune the PBG or PSG regions. So far, irreversible<sup>7</sup> and reversible<sup>8</sup> spectral tuning was demonstrated only in synthetic opal PhC structures. Neither mechanical properties of laser-polymerized microstructures nor mechanical tuning of their optical response have been addressed with respect to the tunability of PBG or PSB so far. In this work, we study the mechanical properties and deformability of 3D PhC structures having woodpile<sup>9</sup> and spiral architectures<sup>10,11</sup> fabricated by DLW in the commercial photoresist SU-8. Elastic properties determined from the measured stress-strain curves, together with theoretical modeling of the optical properties, suggest that a substantial spectral tunability is obtainable with these structures in their elastic regime.

Several 3D PhC structures were fabricated by femtosecond DLW. Descriptions of the optical setup, SU-8 samples, and their processing conditions can be found in our earlier works<sup>1,12,13</sup>.

The architectures of woodpile (W),<sup>9</sup> square spiral (S),<sup>11</sup> and circular spiral (C) PhC structures are illustrated schematically in Fig. 1(a). Detailed descriptions of these archi-

tectures can be found in the above references. Specific to the structures fabricated by DLW is the ellipsoidal elongation of the recorded features along the direction of the fabricating laser beam. Parameters of the fabricated samples are given in the caption of Fig. 1.

The mechanical response of the structures was tested by applying a flat-punch indenter with a micrometer diameter along the  $z$  axis using a NanoIndenter XP (MTS Company),

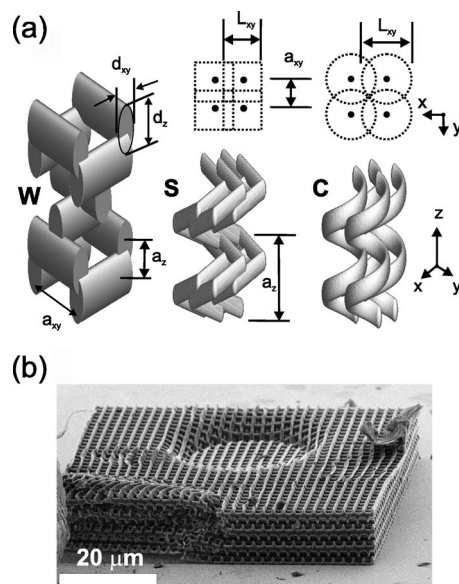


FIG. 1. (a) Schematic explanation of woodpile (W), square spiral (S) and circular spiral (C) architectures, and their parameters. For W, rod-to-rod distance within the layer  $a_{xy}=2.0\ \mu\text{m}$ , layer-to-layer distance  $a_z=0.65\ \mu\text{m}$ , and total number of layers  $N=12$ . For spiral structures, these parameters are redefined. For both S and C,  $a_{xy}=1.0\ \mu\text{m}$  is the period of a square lattice in the  $x$ - $y$  plane on which spirals are centered, and  $a_z=2.64\ \mu\text{m}$  is the vertical period of spirals. For S,  $L_{xy}=1.5\ \mu\text{m}$  denotes the projection of a straight spiral segment on the  $x$ - $y$  plane, for S,  $L_{xy}=1.5\ \mu\text{m}$  is the spiral diameter. Total height of the S and C samples comprises  $N=4$  spiral periods. All structures consist of ellipsoidal SU-8 features elongated in the  $z$ -axis direction (parallel to the laser beam during the DLW) have diameters  $d_{xy}\approx 400\ \text{nm}$  and  $d_z\approx 960\ \text{nm}$ , and on the  $x$ - $y$  plane occupy an area of  $60\times 60\ \mu\text{m}^2$ . (b) SEM micrograph of a woodpile structure fabricated on a glass substrate. The circular impression at the center is left by the flat punch during the tests that exceeded the elastic deformation limit.

<sup>a)</sup>Electronic mail: misawa@es.hokudai.ac.jp.

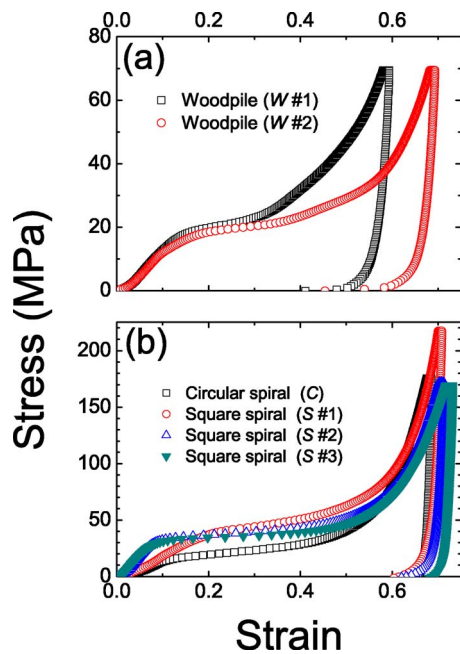


FIG. 2. (Color online) Stress-strain characteristics for (a) woodpile structures, and (b) square and circular spiral structures.

and recording the displacement. Figure 1(b) shows a scanning electron micrograph of a woodpile PhC. Overall fabrication quality can be assessed by examining its periphery. The circular impression seen at the center is due to plastic deformation that was ultimately induced by the flat punch.

The stress-strain curves of several PhC samples are presented in Fig. 2. Significant differences that can be seen in Fig. 2 between the responses of nominally identical samples. These are most likely due to random size variations of the recorded features caused by mechanical instabilities of the DLW setup and laser intensity fluctuations. Nevertheless, woodpiles generally have the lowest structural modulus, whereas circular and especially square spirals have a higher rigidity. Table I lists parameters of the structures determined from the stress-strain curves.

The qualitative mechanical behavior of all samples is similar. At strains below about 10%, the stress increases linearly, signifying the region of reversible elastic deformation, most likely due to bending of SU-8 rods; the slope of the stress-strain curves in this elastic regimes is the structural modulus  $E$  (see Table I). At higher strains, elastic collapse occurs at the stress  $\sigma_{el}$ , followed by densification of the structure. Deformations above  $\sigma_{el}$  are largely plastic and irreversible. Structural collapse most likely occurs via a combination of elastic buckling and the formation of plastic

TABLE I. Parameters extracted from compression tests, ( $E$ ) structural modulus, ( $\sigma_{el}$  and  $\epsilon_{el}$ ) elastic collapse stress and strain, respectively, and ( $\Delta z$ ) height decrease prior to elastic collapse.

Sample	$E$ (MPa)	$\sigma_{el}$ (MPa)	$\epsilon_{el}$ (%)	$\Delta z$ ( $\mu\text{m}$ )
W No. 1	170 $\pm$ 5	17.9	12.7	0.4
W No. 2	147 $\pm$ 5	17.5	13.8	0.44
S No. 1	258 $\pm$ 11	37.3	17.5	1.43
S No. 2	528 $\pm$ 14	32.8	7.9	0.77
S No. 3	494 $\pm$ 17	32.5	7.5	0.71
C	191 $\pm$ 8	15.8	11.4	1.18

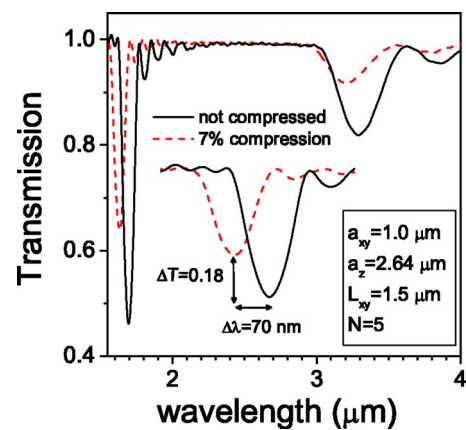


FIG. 3. (Color online) Optical transmission of square spiral structures calculated by FDTD technique before and after the compressive deformation by 7% along the  $z$ -axis direction. Parameters of the spiral are indicated in the plot. The inset shows in detail the attenuation regions near 1.7  $\mu\text{m}$  wavelength.

hinges. Finally, as the strain increases even further, a steep stress-strain response signifies that the cells have collapsed to such an extent that opposite sides touch and further strain compresses the solid SU-8 rod material.

The observed response is similar to that of foams or lattices where bending deformation is dominant.<sup>14</sup> In these systems, structural modulus and elastic collapse stress increase, while densification stress decreases with an increase in relative density.<sup>14,15</sup>

Reversible compression of PhC structures along the  $z$  axis by approximately 10% should induce a blueshift of comparable magnitude of the PSG regions existing along the same direction. As, at present, it is difficult to verify this fact experimentally, the spectral tunability was assessed from theoretical optical transmission calculations before and after the compression. For this, finite-difference time-domain (FDTD) analysis was used. The calculations were done using FDTD SOLUTIONS software (from Lumerical), assuming parameters of the structures similar to those of the fabricated samples. Figure 3 shows the calculated transmission spectra of a square spiral structure before and after the compression by 7%, which is below the elastic limit in all square spiral samples. Parameters of the model structure used for the calculations are indicated in the figure. The calculated spectra reveal optical attenuation regions at the wavelengths of about 3.5  $\mu\text{m}$  and 1.6–1.7  $\mu\text{m}$ , which correspond to a fundamental and a second-order PSG regions, respectively.<sup>2,16</sup> Both PSG regions exhibit notable blueshifts due to the deformation. From a practical viewpoint, the second-order PSG is more interesting due to its spectral proximity to the optical telecommunications spectral range (1.3–1.5  $\mu\text{m}$ ), where coupling of optical radiation in and out of the small PhC samples as well as spectral measurements can be conveniently performed using tools (e.g., optical fibers, lasers, and spectrum analyzers) available in the telecommunications industry. The inset in Fig. 3 emphasizes that elastic compression leads to a blueshift of the second-order PSG by approximately 70 nm ( $\approx 2.7\%$ ).

Hence, mechanical tuning of PhC structures recorded in SU-8 by DLW seems to be a realistic goal for experimental investigations in the near future. It may also be possible to improve the elastic performance of these structures. The elastic response depends on the ratio between the spatially

averaged density  $\langle\rho\rangle$  of the structure and the density of monolithic SU-8  $\rho_s$  (the latter value should take into account nonuniform density of SU-8 features fabricated using Gaussian laser beams<sup>17,18</sup>). The structural modulus generally scales with the ratio  $\rho_r=\langle\rho\rangle/\rho_s$  as  $E\sim E_s\times\rho_r^2$ ,<sup>14,15,19</sup> where  $E_s$  is the Young modulus of monolithic SU-8. Thus, the elastic response can be controlled via the relative display of SU-8 filling fraction.

In conclusion, we have investigated the mechanical properties of periodic polymeric microstructures fabricated by DLW in photoresist SU-8. Stress-strain tests conducted on 3D PhC structures having woodpile and spiral architectures indicate that their overall mechanical response is similar to that found in foams and lattices. All of the investigated structures exhibit an elastic deformation regime for strain up to about 10%. According to numerical FDTD simulations conducted during this work, this regime allows reversible mechanical tuning of the PSG wavelength at infrared wavelengths within the range of tens of nanometers (or a relative range of about 3%), thus illustrating the possibility to exploit the relationship between mechanical and optical properties of PhC structures, for example, in tunable PhC structures or in PhC-based optical strain or position sensors.

The authors thank Dr. S. Enders and Dr. S. Orso, Max Planck Institute for Metals Research, Stuttgart, Germany for experimental assistance with mechanical testing and scanning electron microscopy. S.J. acknowledges financial sup-

port provided by a Grant-in-Aid from the Ministry of Education, Science, Sports, and Culture of Japan (19360322.)

- <sup>1</sup>V. Mizeikis, K. K. Seet, S. Juodkazis, and H. Misawa, *Opt. Lett.* **29**, 2061 (2004).
- <sup>2</sup>K. K. Seet, V. Mizeikis, S. Matsuo, S. Juodkazis, and H. Misawa, *Adv. Mater. (Weinheim, Ger.)* **17**, 541 (2005).
- <sup>3</sup>H.-B. Sun, S. Matsuo, and H. Misawa, *Appl. Phys. Lett.* **74**, 786 (1999).
- <sup>4</sup>H. Okamura, *Proc. SPIE* **6374**, 637401 (2006).
- <sup>5</sup>S. Juodkazis, V. Mizeikis, and H. Misawa, *Adv. Polym. Sci.* (published online October 27, 2007).
- <sup>6</sup>J. D. Joannopoulos, R. D. Meade, and J. N. Winn, *Photonic Crystals: Molding the Flow of Light* (Princeton University Press, Princeton, NJ, 1995), p. 184.
- <sup>7</sup>A. Z. Khokhar, R. M. De La Rue, K. Run, Z.-Y. Li, and N. P. Johnson, *J. Opt. A, Pure Appl. Opt.* **9**, 446 (2007).
- <sup>8</sup>H. Fudouzi and T. Sawada, *Langmuir* **22**, 1365 (2006).
- <sup>9</sup>K. M. Ho, C. T. Chan, C. M. Soukoulis, R. Biswas, and M. Sigalas, *Solid State Commun.* **89**, 413 (1994).
- <sup>10</sup>A. Chutinan and S. Noda, *Phys. Rev. B* **57**, R2006 (1998).
- <sup>11</sup>O. Toader and S. John, *Science* **292**, 1133 (2001).
- <sup>12</sup>S. Juodkazis, V. Mizeikis, K. K. Seet, M. Miwa, and H. Misawa, *Nanotechnology* **16**, 846 (2005).
- <sup>13</sup>K. K. Seet, V. Mizeikis, S. Juodkazis, and H. Misawa, *J. Non-Cryst. Solids* **352**, 2390 (2006).
- <sup>14</sup>M. F. Ashby, *Philos. Trans. R. Soc. London, Ser. A* **364**, 15 (2006).
- <sup>15</sup>M. F. Ashby, E. Evans, N. A. Fleck, L. Gibson, J. W. Hutchinson, and H. N. G. Wadley, *Metal Foams: A Design Guide* (Butterworth Heinemann, Oxford, 2000), p. 251.
- <sup>16</sup>M. Straub and M. Gu, *Opt. Lett.* **27**, 1824 (2002).
- <sup>17</sup>M. Miwa, D. Kazutika, Y. Satoru, T. Shigeki, K. Yasuhiro, and K. Reizo, *Proc. SPIE* **5719**, 6 (2005).
- <sup>18</sup>T. Choi, J.-H. Jang, C. K. Ullal, M. C. Lemieux, V. V. Tsukruk, and E. L. Thomas, *Adv. Funct. Mater.* **2006**, 1324 (2006).
- <sup>19</sup>L. J. Gibson and M. Ashby, *Cellular Solids: Structure and Properties*, 2nd ed. (Cambridge University Press, Cambridge, 1997), p. 510.